Int J Thermophys (2010) 31:2159–2175
DOI 10.1007/s10765-010-0890-x

High-Temperature Vibrational Properties and Melting Curve of Aluminum

N. K. Bhatt · B. Y. Thakore · P. R. Vyas · A. R. Jani

Received: 12 February 2010 / Accepted: 16 November 2010 / Published online: 1 December 2010

Abstract The mean-field theory due to Wang and Li (Phys Rev B 63:196, 2000) to calculate the effective mean potential experienced by vibrating ions in a crystal is used to compute the ion-motional free energy. An improvement is sought by treating the parameter λ, entering an expression of the mean-field potential (MFP), as a free parameter for the case of aluminum. Although a corresponding expression for the Grüneisen parameter (γ) is significantly different then the known cases, namely, those due to (i) Slater, (ii) Dugdale and MacDonald, (iii) free volume theory, and (iv) Barton and Stacey, its value is very close to the experimental result. Significant improvement is observed for high-temperature thermodynamics of aluminum with the new choice of λ, or equivalently γ. Also, the present improved scheme is extended to measure the vibrational response of the crystal. Recently, Bhatt et al. (Philos Mag 90:1599, 2010) have demonstrated that the mean frequency (ω') calculated by the MFP approach in conjunction with the density-dependent local pseudopotential suffices to characterize the crystal at finite temperatures. Relating ω' to the Debye frequency, vibrational properties like the Debye temperature, the mean-square displacement, and entropy are obtained as a function of temperature. Further, a generalized melting law is derived by combining the MFP approach to Lindemann's law, where the effect of different choices of the parameter λ is now explicitly included into the description. Results so obtained for different physical properties are analyzed and discussed in the light of recent first principles and experimental findings.

N. K. Bhatt (✉) · B. Y. Thakore · A. R. Jani
Department of Physics, Sardar Patel University, Vallabh Vidyanagar, 388120 Gujarat, India
e-mail: bhattnisarg@hotmail.com

P. R. Vyas
Department of Physics, Gujarat University, Ahmedabad, 380009 Gujarat, India

Keywords Aluminum · Debye temperature · Grüneisen parameter · Mean-square displacement · MFP · Melting curve

1 Introduction

Vibration of atoms in a crystal is a key ingredient to understand almost all lattice dynamical properties including thermodynamics. A quantized vibrational frequency $\omega_{\vec{q},S}$ having a wave vector $\vec{q}$ and three modes of polarization $S(=L,\ T_1,\ T_2)$ is distributed statistically among different modes of vibrations. In principle, it is required to know the phonon density of states $g(\omega)$ (p-dos) and phonon dispersion curves (pdc) to deduce vibrational properties at a given physical condition. This is computationally quite demanding, as a complete description of $g(\omega)$ would be obtained only if one knows all the frequency moments $\omega(n)$ (see Ref. [1]), which is defined as $3\,[\omega\,(n)]^n = \int_0^{\omega_{\max}} \omega^n g(\omega)\mathrm{d}\omega$, with $n > -3$. And hence computationally, it is always difficult to estimate the high-temperature ion-motional contribution to the total free energy. There remains a question as how to incorporate the effect of temperature into the description in general and the vibrational contribution to the total free energy at finite temperatures in particular.

To circumvent the computational complexity, the concept of the mean-field theory (MFT) is frequently used. The MFT is used to calculate an average or mean potential experienced by a wanderer atom in the presence of surrounding particles. In the past, different philosophies were used to compute the mean-field potential (MFP): free volume theory [2–6], Debye–Grüneisen theory [7], classical cell-model [8], and 0 K isotherm-based MFP [9,11–21]. Wang and his coworkers [9,10,18–20], and others [11–17,21] have proposed a method of modeling the vibrational free energy in terms of the 0 K total energy from the concept of the MFP approach. The concept of the MFP due to Wang and co-workers does not require detailed electronic band structure calculations over the complete density range of interest. It was shown that the high-T, P properties can be mapped through the relevant parameters of ambient conditions only. In Ref. [12], an alternative approach has been proposed to obtain an analytical MFP within the free volume theory and the nearest-neighbor pair-wise interaction assumption using a Lennard-Jones (LJ) potential. Its validity has been tested and confirmed based on the Vinet equation of state for rare-gas, alkali-halide, and metallic solids. Also, the concept of the MFP was modified to more general cases [13], where the effect of the structural parameters, varying with volume, on the total free energy was taken into account. This was applied to obtain the thermodynamics of low symmetry or complex structure crystals, taking beryllium as a prototype. Bhattacharya and Menon [14] have calculated the ionic free energy using the scaled binding energy. They suggested an improvement over the MFP calculated by Wang and Li [9] and Bhatt et al. [21], if the parameter λ is treated as a free parameter. (A detailed discussion regarding the parameter λ and its effect on different properties is given in the next section.) Their proposal summarizes good results for several thermodynamic properties of close-packed metals including the shock Hugoniot and high-pressure melting curve, and to somewhat lesser extent, structural phase diagrams of Fe, Zr, and Ti. They have compared and analyzed their MFP-based predictions with the Debye–Grüneisen

theory within the same scaled binding energy formalism and with experiments. In another recent study [17], we have examined the physical significance of the MFP approach in conjunction with the local pseudopotential for fcc-Sr. We demonstrated that the results for high-temperature frequency shifts calculated through a pdc and p-dos within the quasiharmonic approximation (QHA) are very similar to the one estimated through the MFP approach, and with a better account of intrinsic anharmonism by the MFP scheme. This observation also implies that the mean frequency calculated by the MFP approach is sufficient to characterize the crystal in the high-T and high-P regime.

While the MFP approach is robust, it is employed to reexamine the thermodynamics of aluminum and to obtain some vibrational properties. The objectives of the present work are twofold: (i) treating λ as an adjustable parameter, find the value of λ (which determines the Grüneisen parameter, as described in the next section) that gives the best description of aluminum at high temperatures and (ii) extending the MFP approach to estimate the Debye temperature on general physical grounds. Since a characteristic temperature (θ) is related to the melting temperature in the Debye model, hence, now it shall be possible to derive the melting law on this general grounds. We apply this scheme to trivalent fcc-Al as a case study, and the estimated characteristic temperature is used to estimate the mean-square atomic displacement and high-pressure melting curve within the generalized Lindemann's criterion.

In the following parts of this paper, over and above the formal aspect of computations, we have presented results for some anharmonic properties, temperature variations of Debye temperature, entropy, mean-square displacement (MSD), and high-pressure melting curve. These results are also compared and discussed with the other reported results. In the last section, we give a short summary and conclusion.

2 Theory and Formulation

2.1 Choice of Parameter λ in MFP

As noted earlier, different authors have used different means to construct the MFP [2–21], but we follow the one due to Wang and co-workers in conjunction with the local pseudopotential due to Fiolhais et al. [22,23]. Assuming the vibration of the lattice ion is symmetrical with respect to its equilibrium position, Wang and Li [9] have proposed an analytical form for the MFP, as given by

$$g(r, \Omega; \lambda) = \frac{1}{2}\left[E_{\mathrm{C}}(a_0 + r) + E_{\mathrm{C}}(a_0 - r) - 2E_{\mathrm{C}}(a_0)\right] + \left(\frac{\lambda}{2}\right)\left(\frac{r}{a_0}\right)\left[E_{\mathrm{C}}(a_0 + r) - E_{\mathrm{C}}(a_0 - r)\right], \quad (1)$$

where r is the distance that the lattice ion deviates from an equilibrium position and a_0 is the lattice constant with respect to volume Ω. Wang and Li have shown that the physical significance of the MFP is appreciated from the second-order Taylor expansion of Eq. 1 in r, which gives different equations for the Grüneisen λ corresponding to different choices of λ;

$$\gamma(\Omega) = \frac{1}{3}(\lambda - 1) - \frac{\Omega}{2}\left[\frac{\frac{\partial^2 (P_C \Omega^{2/3(\lambda+1)})}{\partial \Omega^2}}{\frac{\partial (P_C \Omega^{2/3(\lambda+1)})}{\partial \Omega}}\right]. \tag{2}$$

Here, P_C represents the cold pressure. Equation 2 gives expressions for the Grüneisen parameter due to Slater [24], due to Dugdale and MacDonald [25], and the one due to the free volume theory of Vaschenko and Zubarev [5,6] corresponding to $\lambda = -1, 0, +1$, respectively. Formally, Eq. 2 is equivalent to

$$\gamma(\Omega) = -\frac{1}{6} - \frac{1}{2}\frac{\mathrm{d}\ln\left(B_T - \frac{2t}{3}P_C\right)}{\mathrm{d}\ln\Omega}, \tag{3}$$

with $\lambda \rightarrow t - 1$. In general, however, λ or t is not constant [26–28]. For example, Barton and Stacey [26], through their MD study for cubic crystals, suggested $t = +2.35$ or $\lambda = +1.35$ while improving the defect of the free-volume formula for the Grüneisen γ. Whereas, Burakovsky and Preston [27] have shown that at ultrahigh pressure $t \rightarrow \frac{5}{2}$. These studies clearly reveal that the parameter t or λ, which in turn determines the Grüneisen parameter, should be treated as a free parameter as long as its choice gives a better thermal description for a given material. Illustrating this fact, Bhattacharya and Menon [14] have examined this point within the MFP formalism, and have proposed that for the case of fcc-Al, either $\lambda = -2$ or $t = -1$ value gives correct thermophysical properties at high temperatures. While for other metals, they retain the value of λ as either -1 or $+1$. We also in the present study examined different choices of λ and found that $\lambda = -2$ is the suitable choice for trivalent Al, in agreement with Bhattacharya and Menon.

For non-magnetic simple metals, the total or Helmholtz free energy can be expressed by the following equation:

$$F(\Omega, T; \lambda) = E_C(\Omega) + F_{ion}(\Omega, T; \lambda) + F_{eg}(\Omega, T). \tag{4}$$

Here, E_C represents the static total energy at 0 K which is calculated within the framework of pseudopotential theory [22,23] corrected to second order in energy, while F_{eg} is the free energy due to electronic excitation. (See Refs. [15,16,21] for computational details.) The vibrational free energy due to lattice ions within the MFP formalism is given as follows:

$$F_{ion}(\Omega, T; \lambda) = -k_B T\left[\left(\frac{3}{2}\right)\ln\left(\frac{mk_B T}{2\pi\hbar^2}\right) + \ln\{v_f(\Omega, T; \lambda)\}\right], \tag{5}$$

with

$$v_f(\Omega, T; \lambda) = 4\pi\int \exp\left[\frac{-g(r, \Omega; \lambda)}{k_B T}\right] r^2 \mathrm{d}r. \tag{6}$$

By calculating the Helmholtz free energy $F(\Omega, T; \lambda)$ using Eq. 4, as an explicit function of the atomic volume ($\equiv$ pressure) and temperature, it is now straightforward to obtain different anharmonic physical properties following text-book equations.

2.2 Extension of MFP

It is customary to define the equivalent characteristic temperature $\theta = \frac{\hbar\omega_{\vec{q},S}}{k_B}$ for the phonon frequency. In this regard, the characteristic temperature θ is the measure of the vibrational response of a crystal. However, many temperature- and/or pressure-dependent properties do not depend on the precise value of $\vec{q}$ or S. This allows one to simplify the description of p-dos, e.g., Debye and Einstein models [1]. Both are single-parameter models, which can be fitted to give the correct average of ω^n. The generalized Debye model, like the conventional Debye model, assumes ω^2 behavior for $g(\omega)$ but with different Debye cut-off frequencies, $\omega_D(n)$, chosen such that the model correctly reproduces the average of ω^n for the true $g(\omega)$. While in the Einstein model, correlations between atomic vibrations are ignored and $g(\omega)$ is defined through a single frequency, the so-called Einstein frequency, ω_E, such that $g(\omega) \sim \delta(\omega - \omega_E)$. In the classical regime, i.e., at temperatures above the characteristic temperature, it can be expected that the Einstein model should give a correct description of the dynamical response due to weakening of the correlations among vibrating atoms. Much in the spirit of the Einstein model, the essence of the MFP approach is also to assume that each atom in the crystal vibrates with *some* mean or average (single) frequency ω'. Indeed, at elevated temperatures ($T > \theta_D$; the Debye temperature), one may expect weakening of atomic correlations and the use of the mean-field approach is justified. In a recent paper [17], we have examined this point and calculated several thermodynamic properties for strontium in a high-T and high-P environment including finite temperature frequency shifts, and this validates the use of the MFP and pseudopotential coupling scheme. The characteristic temperature obtained by the MFP approach is used to define a Debye temperature along the line suggested by Wang [19];

$$\theta_D = \sqrt{3}\frac{\hbar}{k_B}\left[\frac{k(\Omega, T)}{2m}\right]^{\frac{1}{2}}, \tag{7}$$

where $k(\Omega, T)$ is regarded as a generalized force constant [18,21], and is given by

$$k(\Omega, T; \lambda) = \frac{1}{R^{2\lambda}}\frac{\partial}{\partial R}\left(R^{2\lambda}\cdot\frac{\partial F(\Omega, T)}{\partial R}\right). \tag{8}$$

Here, R is the corresponding atomic radius and λ is now -2. With Eq. 7 in Eq. 8, the Debye temperature is

$$\theta_D(\lambda) = \sqrt{3}\frac{\hbar}{k_B}\left[\frac{1}{2m}\left(\frac{\partial^2 F(\Omega, T)}{\partial R^2} + \frac{2\lambda}{R}\cdot\frac{\partial F(\Omega, T)}{\partial R}\right)\right]^{\frac{1}{2}}. \tag{9}$$

For special cases of either $\lambda = 0$ or under a zero-pressure condition, Eq. 9 reduces to the one that was given in Ref. [19]. Here, the first term corresponds to the radial part of the force constant while the second term is a tangential component of the force constant. Equation 9 can be viewed as a general case of θ_D which is usually given in terms of the pair potential, see the Appendix. In the above equation,

pre-factor $\sqrt{3}$ is arbitrary. In Ref. [17], we found that a characteristic frequency corresponding to the generalized force constant (Eq. 8), is lower by a constant factor, roughly $\sqrt{3}$, compared to the Debye frequency which was calculated from the p-dos within QHA. We found similar results for other metals too, which justifies the presence of $\sqrt{3}$ in Eqs. 7 or 9. The advantage of Eq. 9 over the conventional definition of the Debye temperature (Eq. A1) is twofold: (i) Equation 9 incorporates the effects of temperature and pressure through the total free energy (F) in an unambiguous manner. It is claimed [17,20] that the MFP approach gives a better account of anharmonism in lattice vibrations in the high-T and high-P regime compared to the conventional p-dos based methods either within the harmonic approximation (HA) or the QHA. (ii) Equation 9 provides the quantitative assessment of the philosophies involved in determining the Grüneisen parameter through parameter λ. In a previous study [21], we have also noted that the volumetric thermal expansion is highly sensitive to the choice of λ and, therefore, $\theta_{\mathrm{D}}(\lambda)$ will be, since a major contribution to $\theta_{\mathrm{D}}(\lambda)$ comes from the coefficient of thermal expansion [29,30].

The MSD in the high-T condition, in the Debye treatment, is expressed as $\langle u^2 \rangle \approx \frac{9\hbar^2 T}{mk_{\mathrm{B}}\theta^2}$, where θ is now given by Eq. 9. According to Lindemann [31], melting initiates when $\langle u^2 \rangle = C_{\mathrm{L}} R^2$, where C_{L} is known as Lindemann's constant. Combining these equations, the high-pressure melting curve within the MFP approach is now made to depend on the choice of λ, apart from the model used to evaluate E_{C} in Eqs. 1 and 4. Thus, we have modified the previous melting relation [18] to include the pressure term or tangential component as well, whose magnitude is governed by the value of λ;

$$T_{\mathrm{m}} = C' R^2 \left(\frac{\partial^2 F(\Omega, T_{\mathrm{m}})}{\partial R^2} + \frac{2\lambda}{R} \cdot \frac{\partial F(\Omega, T_{\mathrm{m}})}{\partial R} \right). \tag{10}$$

At this juncture, we also recall the elegant work of Wang et al. [18], and the melting relation given by them is just the special case $\lambda = 0$ of above equation. Following their procedure, the new constant C' can be determined from a fit to the zero-pressure experimental melting temperature and from a knowledge of the total free energy $F(\Omega, T_{\mathrm{m}})$ at melting. Once C' is fixed, the melting temperature at a given pressure can be computed consistently through Eq. 10 for different choices of λ. In the present case, $\lambda = -2$.

3 Results and Discussion

Recently, Bhattacharya and Menon [14] have demonstrated that λ in Eq. 1 may be treated as an adjustable parameter, and for the case of aluminum, its value is -2. Following Bhattacharya and Menon, we too have considered the case for $\lambda = -2$, and following the zero-pressure condition at different temperatures, the volumetric thermal expansion is calculated and plotted in Fig. 1. The computed value of the thermal expansion coefficient at ambient conditions is $6.997 \times 10^{-5}\ \mathrm{K}^{-1}$, which is in excellent agreement with the experimental value of $6.76 \times 10^{-5}\ \mathrm{K}^{-1}$, and remains within 8 % up to the melting temperature. Our previously published results [21] are also compared along with experimental [32] and theoretical estimates due to Wang and Li [9]. These

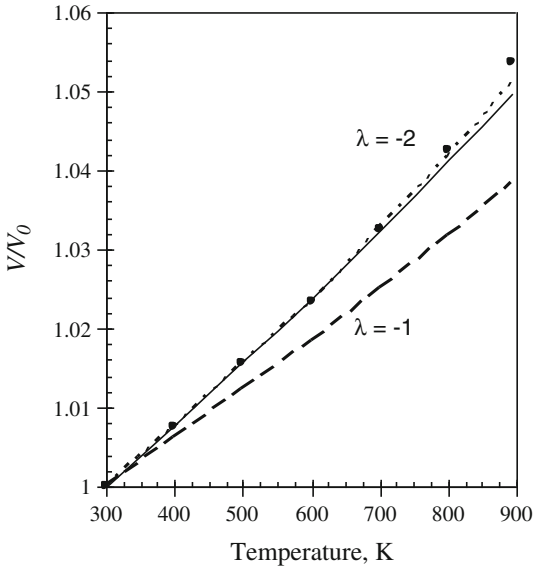

Fig. 1 Relative volume thermal expansion, $\lambda = -2$ case (*continuous line*) and $\lambda = -1$ case (*long-dashed line*), are compared with experimental [32] findings (*circles*) and theoretical estimates due to Wang and Li [9]

authors have calculated E_C in Eq. 4 using the full-potential linearized augmented plane wave (FP-LAPW) method within the generalized gradient approximation (GGA) for an exchange and correlation functional. Their results are also in very good agreement with experiments, even if they considered $\lambda = -1$. Our present estimate ($\lambda = -2$) is showing quantitative improvement compared to the previous results, and therefore confirm the assertion made by Bhattacharya and Menon. These results reveal that the choice of λ is subjective to the material and also to the model applied to calculate E_C, which in turn is required to estimate F_{ion}.

To validate the present choice of λ, we have compared the anharmonic contribution to the ionic specific heat at constant volume ($C_V^{\text{ion-an}} = C_V^{\text{ion}} - 3k_B$) with other reported data [9,14,21,33] in Fig. 2. Again the $\lambda = -2$ case is in better agreement compared to the $\lambda = -1$ case [21], though the maximum deviation is still 30 % compared to the experimental value [33] at $T = 900$ K. Nevertheless, it improves by 13 % compared to the results due to Wang and Li. Results due to Bhattacharya and Menon are also very similar to ours. Figures 1 and 2 clearly reveal the sensitivity of parameter λ and, therefore, the Grüneisen γ on these anharmonic properties.

Burakovsky and Preston [27] have proposed an analytical expression to determine the density or volume dependence of the Grüneisen γ. Using the experimental [32] volume or density at different temperatures, we have calculated the Grüneisen parameter as a function of temperature using their analytical expression for the Grüneisen parameter. These results are compared with our estimates for $\lambda = -2$ and $\lambda = -1$ cases along with the experimental results due to Leadbetter [34] and the theoretical results of MacDonald and MacDonald [35] in Fig. 3. The present estimate for $\gamma = 2.105$ is within the range of other data. The major discrepancy observed in the present ($\lambda = -2$) results, and that due to Burakovsky and Preston, is the opposite trend. Their results increase with temperature while ours decrease; however, both

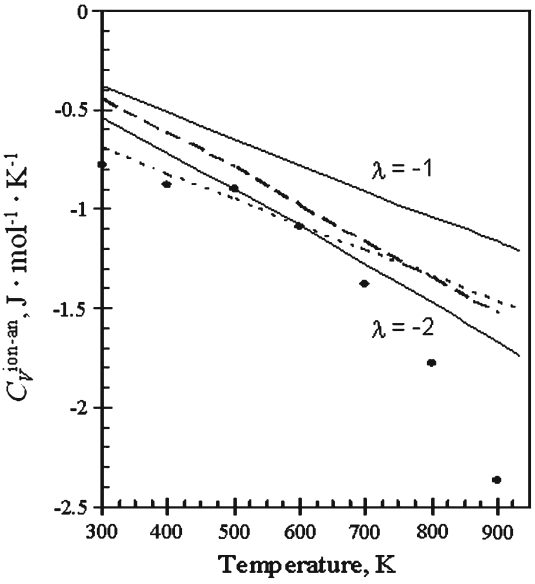

Fig. 2 Anharmonic contribution to ionic specific heat at constant volume is plotted as a function of temperature. Present estimates (*continuous lines*) are compared with experimental [33] data (*circles*) and theoretical calculations due to Wang and Li [9] (*long-dashed line*) and Bhattacharya and Menon [14] (*short-dashed line*)

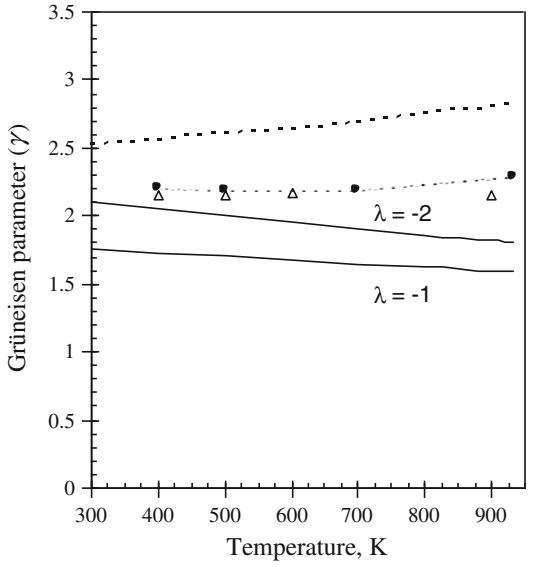

Fig. 3 Present results for Grüneisen parameter (*continuous lines*). Experimental results due to Leadbetter [34] are shown as *circles*, while theoretical findings of MacDonald and MacDonald [35] and those due to Burakovsky and Preston [27] are displayed as *open triangles* and *short-dashed line*, respectively. *Dotted line* connecting experimental findings gives view to eye

show a weak temperature dependence. To resolve this conflict, we believe that the study of thermoelastic properties or, explicitly, the temperature variation of Poisson's ratio involving an intrinsic anharmonism is inevitable. Nevertheless, considering the good overall agreement for several thermodynamic properties in the high-T regime, we retain the $\lambda = -2$ case.

Following Eq. 9, at $T = 0$ K with a zero-pressure condition, the Debye temperature is given by $\theta_0 = \sqrt{3}\frac{\hbar}{k_B}\left[\frac{1}{2m}\cdot\frac{\partial^2 E_C(\Omega)}{\partial R^2}\right]^{\frac{1}{2}}$. The presently calculated value of $\theta_0 = 383.6$ K is in reasonable agreement with the experimental value ($\theta_0 = 428$ K). Its temperature variation is calculated using Eq. 9 for $\lambda = -2$, and the results are depicted in Fig. 4. For convenience, the caloric data based findings for $\theta \rightarrow \frac{T}{T_m}$ due to Rosén and Grimvall [29] are converted to $\theta \rightarrow T$ using the experimental melting temperature ($T_m = 933.5$ K), and compared in Fig. 4. At very low temperatures ($T \ll \theta$), the MFP approach may not be suitable due to correlation effects among atoms. Like most high-temperature theories to estimate the ion-motional contribution, in the MFP formalism the classical partition function for energy calculations is also employed, which is no longer valid at temperatures below the characteristic temperature. Accepting this inherent limitation of the MFP approach and considering the spirit of the paper to study vibrational properties at finite temperatures, the discrepancy in θ at low temperatures may be ignored. But at and above room temperature, our results closely match (within 4 %) the findings due to Rosén and Grimvall. These authors have calculated entropy from the experimental heat capacities (C_P) data [36], and from the resulting entropy, they have estimated the entropy-Debye temperature (EDT) at different temperatures. They have also calculated θ_D from the extrapolated fit to low-temperature Debye-temperature results and using low-temperature p-dos data within the HA. While the latter remains constant and shows no dependence on temperature at finite temperatures, the EDT decreases with temperature due to *softening* of the phonon frequencies. These results clearly demonstrate the inadequacy of HA in the high-T regime, where anharmonic contributions play an imperative role in determining lattice dynamics and related properties. The slope in the EDT $\rightarrow T$ graph is found to be -0.0609 for the intermediate temperature range, but increases to -0.1072 close to melting. We believe that the sharp decrease in θ is due to the rapid increase in C_P [36] at or near melting, again manifesting the importance of anharmonism. The present results give a slope of $\theta \rightarrow T - 0.0632$, indicating a proper account of anharmonicity. Justification for this observation comes from the better thermal expansion accounted for the case $\lambda = -2$. For metals, at the lowest order, i.e., keeping only terms cubic in the crystal Hamiltonian, the major contribution to anharmonism comes from the thermal expansion, and a better account of the thermal coefficient by the case $\lambda = -2$ leads to good results for the entropy and θ. It is to be emphasized that we have not fitted or used any of the experimental quantities in the present study while calculating E_C and thereby F_{ion}, except assuming the zero-pressure condition. Once the potential parameters were obtained at 0 K with a minimization criterion, the rest of the calculations were carried out consistently.

It is also of obvious interest to compare the presently calculated entropy, $S(\Omega, T) = -\frac{\partial F(\Omega,T)}{\partial T}$, with the other first principles and experimental results. Shown in Fig. 5 is the $S \rightarrow T$ graph along with the other estimates. Again closer agreement is observed with the experimental findings [37]. The results for entropy due to Jeong et al. [38] are similar to ours but overestimate compared to the experimental results for the entire range of temperatures. These authors have performed an MD simulation method employing the embedded-atom method (EAM) to calculate the internal energy. Slightly underestimated results in the present study can be explained as follows. It is found that the

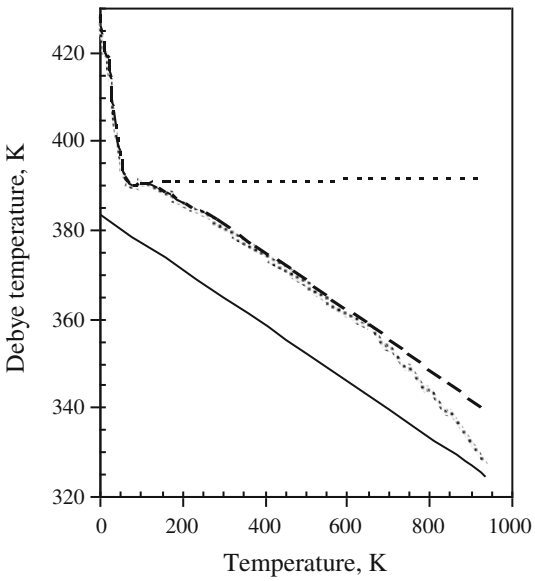

Fig. 4 Present estimate ($\lambda = -2$) for Debye temperature as a function of temperature (*continuous line*) is compared with the results due to Rosén and Grimvall [29]: entropy-Debye temperature (*dotted line*), the fitted 'harmonic' entropy-Debye temperature, i.e., based on low-temperature based phonon density of states (*short-dashed line*), and extrapolated fit to low-temperature Debye data (*long-dashed line*)

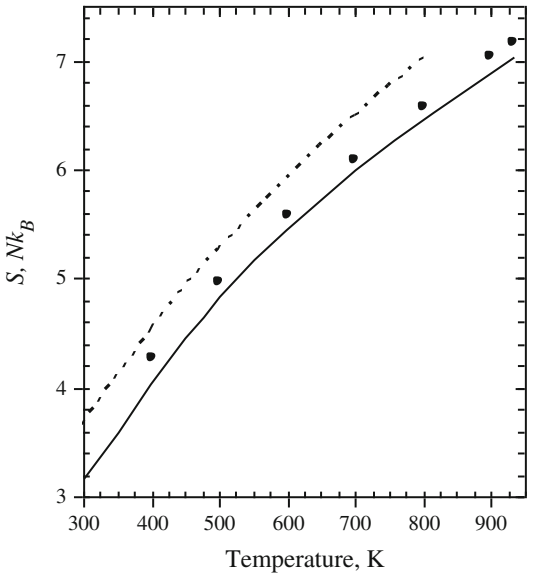

Fig. 5 Temperature variation of entropy for the case $\lambda = -2$ (*continuous line*) is shown. MD results (*short-dashed line*) are from Ref. [38], while experimental points (*filled circles*) are due to Hultgren et al. [37]

volume expansion is better accounted for in the case of $\lambda = -2$, but still it is lower than the experimental volumes. The smaller value of the crystal volume stiffens the phonon modes leading to a smaller entropy. Nevertheless, it is interesting to note that the present results for the entropy when fitted to a logarithmic function of the type $S = A\ \ln(T) - B$ show good correlation (>0.9998) with the calculated results. With A ($= 3.3416\, Nk_{\mathrm{B}}\, \mathrm{K}^{-1}$) and B ($= 15.9710\, Nk_{\mathrm{B}}$) are the constants. A similar

log behavior for the entropy was also proposed by Straub et al. [39] through the MD technique.

Another important anharmonic physical quantity is the MSD of vibrating atoms, $\langle u^2 \rangle$. A knowledge of it is required to obtain the Debye–Waller factor (DWF), which is helpful in determining the intensity profile of X-rays and neutron scattering from the crystal. It has been emphasized [40] that a correct evaluation of $\langle u^2 \rangle$, both in the bulk and surface of crystals, requires investigations of lineshifts and linewidths of phonon modes. While the HA in lattice dynamics is inadequate to observe the temperature dependence of the phonon frequencies, evaluations of anharmonic contributions in the high temperature limit pause challenge. Though a different successful scheme has been proposed in the past [41–44], they are all mathematically demanding and frequent use of them is restricted. Since MSD is related to the Debye temperature, the presently calculated temperature variation of the Debye temperature is used to obtain $\langle u^2 \rangle$ as a function of temperature. The results so obtained are presented in Fig. 6 along with the other theoretical [45,46] and experimental [47–49] findings. The author in Ref. [45] has calculated the atomic MSD of Al and noble metals within HA and QHA, and also by considering anharmonic contributions from the estimated lineshifts and linewidths of the phonon modes. The author has used a force constant model potential to calculate interatomic forces within HA and QHA, whereas anharmonic contributions were considered through the phonon spectral function by including the shifts in phonon frequencies. In the lowest order of anharmonic contributions, shifts in phonon frequencies are due to the thermal expansion, and the third and fourth powers of the atomic displacements from the equilibrium position. It was demonstrated [45] that the inclusion of these latter quantities improves the results quantitatively and justifies the importance of anharmonic effects beyond the volume expansion effects in the high-T regime. More recently, Kagaya et al. [46] have separated the contributions of longitudinal (L) and transverse (T) acoustic modes of vibrations to MSD, and noted that the L-branch is less sensitive to temperature than the T-branch. Better accord of our results with these findings reveals that the present scheme incorporates effects of both the modes accurately. Our results are also in close confirmation to these as well as experimental data [47–49]. At $T = 850\,\mathrm{K}$, our result underestimates the experimental datum [49] by just 1.8 %. Nevertheless, our results are better compared to that evaluated by Zoli [45] employing the QHA and HA, and this confirms the assertion that the MFP approach goes beyond QHA [17,20] and includes the intrinsic anharmonic effects properly. The present results also suggest that the atomic vibrations are non-linear; and close to melting, the magnitude of $\sqrt{\langle u^2 \rangle}$ increases rather rapidly.

Finally, Fig. 7 displays the high-pressure melting relation calculated through the generalized force constant method within Lindemann's criterion and MFP formalism for fcc-Al along with the first principles results [38,50,51] and experimental values [52–54]. Previously, we [21] obtained the melting curve for fcc-Al without considering a pressure term in Eq. 10 and with $\lambda = -1$, and it will not be replicated here. The melting curve obtained using Eq. 10 is in good agreement with the other first principles data when λ is taken as -2. Alfè et al. [50] have determined the melting curve of fcc-Al up to a pressure of 150 GPa using a first principles thermodynamic integration method with the VASP (Vienna *ab-initio* simulation package) code combined

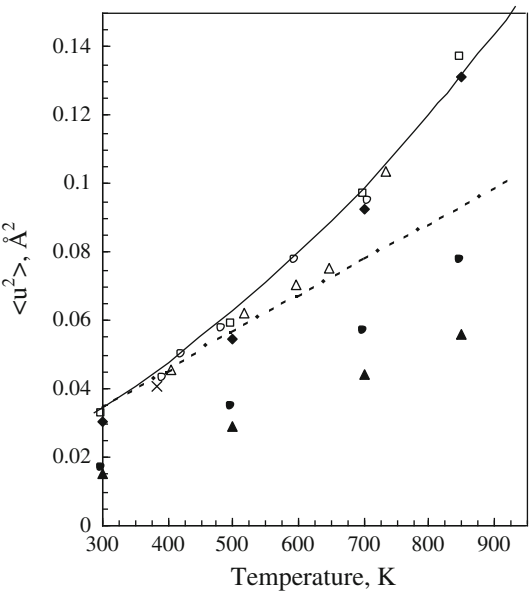

Fig. 6 Mean-square displacement versus temperature is plotted for the case $\lambda = -2$ (*continuous line*). Theoretical results: due to Zoli [45] using HA (*solid triangles*), using QHA (*solid circles*), and by including anharmonic effects (*solid diamonds*), and due to Kagaya et al. [46] (*short-dashed line*). Experimental results (*open circles*, *open triangles*, *open squares*) are due to Refs. [47–49], respectively

to ultrasoft Vanderbilt pseudopotentials to compute the free energy of the solid state, while the liquid state free energy was obtained with the same technique but employing the LJ potential. These authors have also calculated the entropy, volume, and melting gradient upon melting as a function of pressure. Chisolm et al. [51] have proposed a means for constructing an accurate EOS for elemental solids and liquids from first principles. Their method was based on a decomposition of the Hamiltonian. The resulting free energy contained terms describing the harmonic motion of the nuclei about their lattice sites, thermal excitations of the electrons, anharmonic corrections to the nuclear motion, and interactions between the electron excitations and nuclear motion. While in Ref. [38], the classical MD technique was employed using EAM to study melting of aluminum under shock conditions. Even with good accordance to other experimental and theoretical data (with a maximum deviation of 10.7 % at $P = 200$ GPa) when $\lambda = -2$, it is to be noted that when the second term is ignored in Eq. 10, the predicted melting curve remains too low (22 % at 200 GPa) compared to the first principles findings. This observation certainly emphasizes the importance of the tangential or second term in the melting law. In this regard, it would be interesting to discuss a very same approach due to Wang et al. [18]. In their original work, Wang et al. [18] have derived a similar melting law but without considering the pressure term. Even though they obtained good results for the high-pressure melting curve for some close-packed metals in conflict with our prediction (i.e., requiring a pressure term in the melting relation), this may be explained as follows. They considered the $\lambda = -1$ case, probably, for a better thermal expansion for the metals studied. Our calculation suggest that with $|\lambda| = 1$, the contribution of the second term always remains an order of magnitude less as compared to the radial term at the highest pressure studied. The presence of the second term is best appreciated when λ is greater than unity. It is also

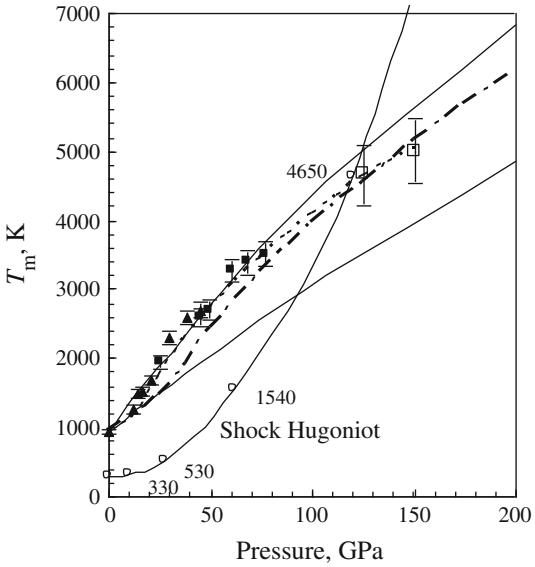

Fig. 7 High-pressure melting curve is presented for case $\lambda = -2$ with (*upper continuous line*) and without (*lower continuous line*) considering a pressure term in Eq. 10. Experimental data: DAC data (*solid triangle*, *solid square*) are from Refs. [52,53], while shock-melting data (*open square*) are due to Shaner et al. [54]. Theoretical results are due to Alfè et al. [50] (*short-dashed line*) and that due to Chisolm et al. [51] (*long-short dashed line*). Also shown is the presently estimated results for temperatures along the principal Hugoniot. Hugoniot temperatures for few data points are also displayed

found [10,14,18,55] that the equation of state is less sensitive to the choice of λ, and good results for the PV relation were obtained even for the $\lambda = 0$ case [10], but that does not guarantee a correct evaluation of other anharmonic properties. For example, for the case of copper, the melting curve predicted by Wang et al. [18] and GPT-based results due to Moriarty [55] differ above 200 GPa. So, in our opinion, a more stringent test for the choice for λ should be either the thermal expansion effect or specific heats at higher temperatures.

The recent study also reveals that the +ve and −ve signs of the parameter λ basically gives upper and lower bounds for different physical properties, including the melting curve, for a given material and for a given model adopted to determine the 0 K isotherm. As a further check on the applicability of the present scheme in a high-T and high-P environment, we have plotted the Hugoniot temperature (T_H) in Fig. 7. The intersection of the T_H curve with the melting curve (with the pressure term included) is used to estimate the beginning of the melting curve along the principal Hugoniot. We found an intersection at 124 GPa and 4950 K in agreement with MD results [38]. Results in [38,50,51] are all in agreement with each other and are in excellent agreement with the available experimental data. In common, these theoretical studies have considered solid and liquid phases while evaluating the high-pressure melting curve, emphasizing a two-phase melting scheme. But such a two-phase approach is numerically cumbersome even for small atomic systems, and we used the generalized Lindemann's law. Looking to the mathematical simplicity and a fact that we have not included/fitted structural information from the liquid state, our results for the high-pressure melting curve are in agreement with the reported data, and are able to mimic the characteristic fcc melting curve, i.e., an increase in T_m with pressure. Since Al melts from the fcc phase, a high packing fraction and the relative closeness of the Fermi surface (FS) to the boundaries of the Brillouin zone (BZ) in the fcc phase results into strong

interactions of FS with BZ. On compressing the material, this interaction is influenced, and one requires a higher thermal energy to melt the crystal. Good results for T_m are consistent with the prediction due to Lawson [56] that the Lindemann rule is well obeyed for the elements with close-packed structures.

4 Summary and Conclusions

In particular, the mean potential seen by a vibrating lattice ion is modified by treating the parameter λ as a free parameter. Its value is now adjusted to give the best possible description for thermal properties of aluminum at high temperatures. We found that $\lambda = -2$ is the correct choice for fcc-Al, in agreement with the recent study by Bhattacharya and Menon [14]. Good accordance of the thermal expansion coefficient and anharmonic contribution to the ionic specific heat at constant volume is thus obvious. The value of the Grüneisen parameter always depends heavily on the method of obtaining it, and as a result, a set of values is available in the literature. We found its ambient value to be 2.105, within the range of other reported values. Also, in the Mie–Grüneisen theory it is independent of temperature, and its temperature variation remains a subject of question. We found that it decreases by 14 % at melting when $\lambda = -2$. In conflict is the opposite slope in the $\gamma \rightarrow T$ graph for the present results and those due to Burakovsky and Preston [27]; this requires further consideration. Alternatively, one may write the polynomial form for λ (and thereby for γ), which depends on density as suggested by Burakovsky et al. [28] for a proper account of anharmonism as a function of density. We instead stick to the constant value of $\lambda = -2$, and the variation of the Grüneisen parameter with density is obtained within the MFP formalism in a consistent manner. We also derived a formula for the Debye temperature on a general physical basis, which makes it possible to include and explore the effect of different choices of λ and thereby different philosophies to determine the Grüneisen parameter (γ) on different physical properties. The results for vibrational properties like the Debye temperature, MSD, and entropy, and also the melting curve are now depending on the choice of λ. Small discrepancies observed in these results at extreme conditions, i.e., $T > 0.8T_m$, and $P > 125$ GPa, which in our opinion, are due to neglect of vacancy contributions [57]. Vacancies give contributions to the entropy which will give an apparent shift in the Debye temperature due to the excess entropy associated with the softening of the vibration frequencies for atoms close to the vacant site. Good results for the Debye temperature and MSDs show better evaluation of anharmonic effects at high-T, and provide the confirmation that the MFP approach is better compared to the QHA.

A similar conclusion may be drawn from our recent study on fcc-Sr. We [17] have estimated frequency shifts for Sr at high temperatures through the MFP approach, and results are in good accord with those due to QHA, and show a relatively rapid increase close to melting as compared to QHA results. This observation manifests again, that near melting, incorporation of intrinsic anharmonism is important, which is suspect within the QHA. Results for the entropy are also in good agreement with the reported data. Noticeable is the high-pressure melting curve. In particular, we have modified the melting formula proposed earlier by Wang et al. [18] from the general definition

of the Debye temperature, Eq. 9. Now, the melting formula depends explicitly on λ, combined with a pressure term. Results clearly reveal that for the case $\lambda = -2$, the melting curve improves significantly at high pressures compared to the previously reported results [21]. Good results for the melting curve for some metals by Wang et al. [18], without considering the second term in Eq. 10 and with $\lambda = -1$, indicate that the choice of λ also depends on the model chosen to describe E_C. For materials which are properly described by $\lambda = \pm 1$, the contribution of the pressure term is small up to moderate compression, but this is certainly not the case when a higher value of λ is required for a proper account of anharmonicity. And one should include the tangential (second) term in Eqs. 8–10.

In conclusion, we have presented an energy calculation-based numerical approach (MFP + pseudopotential) to calculate several lattice dynamical properties, and the high-pressure melting temperature within the Lindemann's criterion, which is not only computationally simple, but also consistent with other first principle methods. The essence of MFP is to map high-temperature properties using a mean single characteristic frequency or equivalently a characteristic temperature, and is justified during the present calculations. Particularly, it is also found that the present approach is best suited to estimate a high-P melting curve for a system showing no structural phase transition up to the highest pressure. Good results for vibrational properties corroborate that the metal aluminum remains *simple* even up to moderate temperatures and pressures.

Acknowledgments NKB expresses gratefulness to Profs. S. V. G. Menon and M. K. Srivastava, and also to C. Bhattacharya for stimulating discussion on the concept of MFP and the choice of parameter λ during his short visit to BARC, Mumbai. The support given by the UGC, New Delhi under the research project no. F. 34-504\2008 (SR) is also acknowledged.

Appendix

Following Hirschfelder et al. [58], the Debye temperature can be related to the radial and tangential force constants as

$$\theta_D \equiv \left[\frac{1}{m}\sum_{i=1}^{n} n_i (F_T + F_R)\right]^{\frac{1}{2}}, \tag{A1}$$

where n_i is the ith coordination number, m is the mass of an atom, and F_T and F_R are known as the tangential force and radial force constants, respectively. For a pair-wise potential, since the total energy can be calculated as $U \equiv \frac{1}{2}\sum_{i=1}^{n} V(r)$, we may write

$$F_T = \frac{1}{R}\frac{\partial V}{\partial R} \equiv \frac{1}{R}\frac{\partial F(\Omega, T)}{\partial R}, \tag{A2}$$

and

$$F_R = \frac{\partial^2 V}{\partial R^2} \equiv \frac{\partial^2 F(\Omega, T)}{\partial R^2}. \tag{A3}$$

Using these equations, the Debye temperature can be written in terms of the total energy,

$$\theta_{\mathrm{D}} \equiv \left[\frac{1}{2m}\left(\frac{1}{R}\cdot\frac{\partial F(\Omega,T)}{\partial R}+\frac{\partial^2 F(\Omega,T)}{\partial R^2}\right)\right]^{\frac{1}{2}}. \tag{A4}$$

The bracketed value is nothing but the generalized Debye temperature, Eq. 9, with a special case of $\lambda = +1$.

References

1. G. Grimvall, in *Ab Initio Calculation of Phonon Spectra*, ed. by J.T. Devreese, P.E. Van Camp (Plenum, New York, 1983)
2. J.G. Kirkwood, J. Chem. Phys. **18**, 380 (1950)
3. W.W. Wood, J. Chem. Phys. **20**, 1334 (1952)
4. Z.W. Salsburg, W.W. Wood, J. Chem. Phys. **37**, 798 (1962)
5. V.Y. Vashchenko, V.N. Zubarev, Fiz. Trerd. Tela (Leningard) **3**, 886 (1963)
6. V.Y. Vashchenko, V.N. Zubarev, Sov. Phys. Solid State **5**, 653 (1963)
7. V.L. Moruzzi, J.F. Janak, K. Schwarz, Phys. Rev. B **37**, 790 (1988)
8. E. Wasserman, L. Stixrude, R.E. Cohen, Phys. Rev. B **53**, 8296 (1996)
9. Y. Wang, L. Li, Phys. Rev. B **63**, 196 (2000)
10. Y. Wang, D. Chen, X. Zhang, Phys. Rev. Lett. **84**, 3220 (2000)
11. S. Xiang, L. Cai, F. Jing, S. Wang, Phys. Rev. B **70**, 174102 (2004)
12. S. Jiuxun, C. Lingcang, W. Qiang, J. Fuqian, Phys. Rev. B **71**, 024107 (2005)
13. H.F. Song, H.F. Liu, Phys. Rev. B **75**, 245126 (2007)
14. C. Bhattacharya, S.V.G. Menon, J. Appl. Phys. **105**, 064907 (2009)
15. N.K. Bhatt, P.R. Vyas, V.B. Gohel, A.R. Jani, J. Phys. Chem. Solids **66**, 797 (2005)
16. N.K. Bhatt, P.R. Vyas, V.B. Gohel, A.R. Jani, Eur. Phys. J. B **58**, 61 (2007)
17. N.K. Bhatt, P.R. Vyas, A.R. Jani, Philos. Mag. **90**, 1599 (2010)
18. Y. Wang, R. Ahuja, B. Johansson, Phys. Rev. B **65**, 014104 (2001)
19. Y. Wang, Theoretical Studies of Thermodynamic Properties of Condensed Matter Under High Temperature and High Pressure, Ph.D. Thesis, KTH (2004), http://urn.kb.se/resolve?urn=urn:nbn:se:kth:diva-3718
20. Y. Wang, Z.-K. Liu, L.-Q. Chen, L. Burakovsky, R. Ahuja, J. Appl. Phys. **100**, 023533 (2006)
21. N.K. Bhatt, P.R. Vyas, A.R. Jani, V.B. Gohel, Indian J. Phys. **80**, 707 (2006)
22. C. Fiolhais, J.P. Perdew, S.Q. Armster, J.M. MacLaren, M. Brajczewska, Phys. Rev. B **51**, 14001 (1995)
23. C. Fiolhais, J.P. Perdew, S.Q. Armster, J.M. MacLaren, M. Brajczewska, Phys. Rev. B **53**, E 13193 (1996)
24. J.C. Slater, *Introduction to Chemical Physics* (McGraw-Hill, New York, 1939)
25. J.S. Dugdale, D.K.C. MacDonald, Phys. Rev. **89**, 832 (1953)
26. M.A. Barton, F.D. Stacey, Phys. Earth Planet. Int. **39**, 167 (1985)
27. L. Burakovsky, D.L. Preston, J. Phys. Chem. Solids **65**, 1581 (2004)
28. L. Burakovsky, D.L. Preston, Y. Wang, Solid State Commun. **132**, 151 (2004)
29. J. Rosén, G. Grimvall, Phys. Rev. B **27**, 7199 (1983)
30. M. Zoli, Phys. Rev. B **41**, 7497 (1990)
31. F.A. Lindemann, Phys. Z. **11**, 609 (1910)
32. Y.S. Touloukian, R.K. Kirby, R.E. Taylor, P.D. Desai, *Thermophysical Properties of Matter*, vol. 12 (Plenum, New York, 1975)
33. U. Schmidt, O. Vollmer, R. Kohlhaas, Z. Naturforsch. A: Phys. Sci. **25**, 1258 (1970)
34. A.J. Leadbetter, J. Phys. C **1**, 1489 (1968)
35. R.A. MacDonald, W.M. MacDonald, Phys. Rev. B **24**, 1715 (1981)
36. Y.S. Touloukian, *Thermophysical Properties of High Temperature Solid Materials*, vol. 1 (MacMillan Pubs., New York, 1967)

37. R. Hultgren, P.D. Desai, D.T. Hawkins, M. Gleiser, K.K. Kelley, D.D. Wagman, *Selected Values of Thermodynamic Properties of The Elements* (American Society for Metals, Metals Park, OH, 1973)
38. J.-W. Jeong, I.-H. Lee, K.J. Chang, Phys. Rev. B **59**, 329 (1999)
39. G.K. Straub, J.B. Wills, C.R. Sanchez-Castro, D.C. Wallace, Phys. Rev. B **50**, 5055 (1994)
40. G. Armand, P. Zeppenfeld, Phys. Rev. B **40**, 5936 (1989)
41. A.A. Maradudin, A.E. Fein, Phys. Rev. **128**, 2589 (1962)
42. R.C. Shukla, H. Hübschle, Phys. Rev. B **40**, 1555 (1989)
43. M. Zoli, Phys. Rev. B **41**, 7497 (1990)
44. M. Zoli, G. Santoro, V. Bortolani, A.A. Maradudin, R.F. Wallis, Phys. Rev. B **41**, 7507 (1990)
45. M. Zoli, Philos. Mag. Lett. **64**, 285 (1991)
46. H.-M. Kagaya, K. Imazawa, M. Sato, T. Soma, J. Mater. Sci. **33**, 2595 (1998)
47. D.R. Chipman, J. Appl. Phys. **31**, 2012 (1960)
48. E.A. Owen, R.W. Williams, Proc. R. Soc. London, Ser. A **188**, 509 (1947)
49. D.L. McDonald, Acta Crystallogr. **23**, 185 (1967)
50. D. Alfè, L. Vočadlo, G.D. Price, M.J. Gillan, J. Phys.: Condens. Matter **16**, S973 (2004)
51. E.D. Chisolm, S.D. Crockett, D.C. Wallace, Phys. Rev. B **68**, 104103 (2003)
52. R. Boehler, M. Ross, Earth Planet. Sci. Lett. **153**, 223 (1997)
53. A. Hänström, P. Lazor, J. Alloys Compd. **305**, 209 (2000)
54. J.W Shaner, J.M. Brown, R.G. McQueen, in *High Pressure in Science and Technology*, ed. by C. Homan, R.K. MacCrone, E. Whalley (North Holland, Amsterdam, 1984), p. 134
55. J.A. Moriarty, Phys. Rev. B **49**, 12431 (1994)
56. A.A.J. Leadbetter, J. Phys. C **1**, 1489 (1968)
57. B. Grabowski, L. Ismer, T. Hickel, J. Neugebauer, Phys. Rev. B **79**, 134106 (2009)
58. J.O. Hirschfelder, C. Curtiss, R.B. Bird, *Molecular Theory of Gases and Liquids* (Wiley, New York, 1954), p. 1042